Journal of Materials Chemistry A

Accepted Manuscript

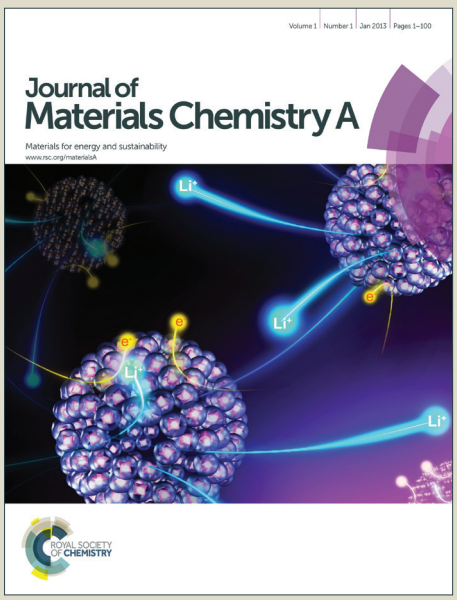

ROYAL SOCIETY OF CHEMISTRY

www.rsc.org/materialsA

Journal of Materials Chemistry A

COMMUNICATION

Direct Insight into Crystallization and Stability of Hybrid Perovskite $CH_3NH_3PbI_3$ via Solvothermal Synthesis†

Received 00th January 20xx,
Accepted 00th January 20xx

DOI: 10.1039/x0xx00000x

www.rsc.org/

Ying Chen,[a] Shuang Yang,[a] Xiao Chen,[a] Yi Chu Zheng,[a] Yu Hou,[a] Yu Hang Li,[a] Hui Dan Zeng,[*b] and Hua Gui Yang,[*a]

Here we report a one-pot solvothermal approach to synthesize the cuboid shaped $CH_3NH_3PbI_3$ single crystals and study the stability of crystallographic planes under solvothermal system. Furthermore, the dissolving phenomenon from specific facets was discovered for the first time. Through careful control of the crystallization and dissolution process, we found that reaction factors including temperature and time, play crytical roles in the crystallization process of perovskite crysals .

Organic-inorganic hybrid materials, particularly the perovskite family, have shown great promise for the applications in field effect transistors, light-emitting diodes, sensors, and photodetectors for more than a decade. The organometal halide perovskites combine the favourable properties of the inorganic semiconductor, namely its excellent charge carrier mobility, with the flexibility and low-temperature processability of the organic material.[1] Since Miyasaka et at used perovskite as sensitizer for the first time demonstrating solar-to-electrical energy conversion efficiency of 3.81% at 1 sun illumination in iodide-based redox electrolyte,[2] the $CH_3NH_3PbX_3$ (X = Cl, Br or I) perovskites have made a breakthrough as the sensitizer of solar cells recently.[3-10] Their high light absorption coefficient and bipolar transport mobility character, which enables the conduction of both electrons and holes, opened a complete new field in photovoltaic devices. A high energy conversion efficiency of 20.1% was confirmed by Korea Research Institute of Chemical Technology (KRICT). Moreover, the perovskite materials have also been a promising candidate for the applications in efficient light emitting diodes (LEDs) and on-chip coherent light sources owning to their high photoluminescence (PL) quantum efficiencies and the wavelength-tunable lasing performances.[11-14]

Since the successful applications of perovskites in various fields, numerous efforts have been devoted to studying the materials. Generally the synthetic methods were hindered by the limited extent of solubility which could be influenced by controlling temperature and the impacts of convective currents that both disturb the ordered growth of the crystals. Recently there are several reports about creating large single crystals.[15-18] These reports mainly pay attention to the photoelectric property of the single crystals, such as carrier diffusion length, hysteresis effect and the trap-state density. Factors such as charge dissociation efficiency, charge transport and diffusion length of charge species are dependent on the crystallinity and size of the perovskite crystals.[19-22] And the above performance have reached the state of the art standard. However, the stability of perovskite has been identified as a critical factor to the commercial viability of perovskite photovoltaic technology. Currently, little is known regarding the crystal growth mechanism as well as the instability of the common crystallographic planes of the as-synthesized crystals. It is crucial to explore the crystallization and stability of perovskites based on the synthesis of high quality crystals. Researches on controlling structure, grain size and crystalline degree remain key scientific challenges for the realization of high performance devices. Therefore, significant importance for $CH_3NH_3PbI_3$ perovskites is the synthesis of high-quality crystals as well as further understanding of the crystal growth and the stability of their common crystallographic planes.

Here we have successfully synthesize high-quality and uniform cuboid shaped perovskite single crystals bounded with (001) and (010) facets under solvothermal conditions. The solvothermal stability of the faceted cuboid perovskite crystals was then systematically investigated in an aqueous environment, and a plausible dissolving kinetic model was also developed. The dissolving effect enhanced with the prolonged time and the increased temperature for perovskite $CH_3NH_3PbI_3$ crystals. The results suggested that the fundamental materials research as shown here, may ultimately help elucidate improved processing conditions leading to thin films of perovskites with optimized crystal parameters and enduring stability, which, in turn, may give rise to enhanced opto-electronic properties.

Powder X-ray diffraction (PXRD) and field emission scanning electron microscopy (SEM) (Figure 1A) were employed to confirm

[a] Key Laboratory for Ultrafine Materials of Ministry of Education, School of Materials Science and Engineering, East China University of Science and Technology, 130 Meilong Road, Shanghai, 200237 (China), E-mail: hgyang@ecust.edu.cn.
[b] School of Materials Science and Engineering, East China University of Science and Technology, 130 Meilong Road, Shanghai, 200237 (China), E-mail: hdzeng@ecust.edu.cn

† Electronic Supplementary Information (ESI) available: [Experimental section, material characterization and supporting figures]. See DOI: 10.1039/c000000x/

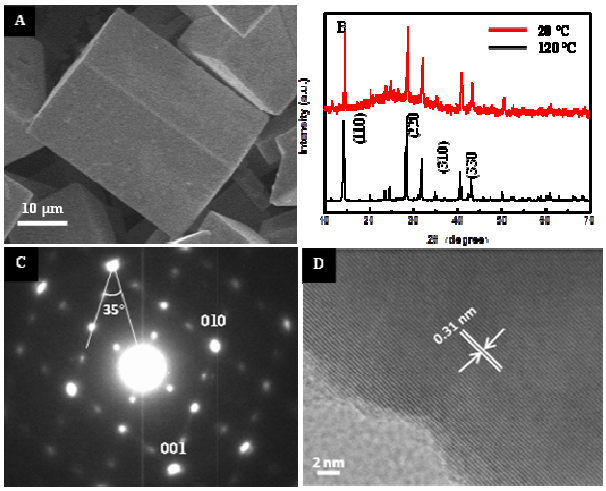

Figure 1. (A) SEM of the perovskite $CH_3NH_3PbI_3$ prepared at 120 °C for 0.5 h. (B) SEM of the perovskite $CH_3NH_3PbI_3$ prepared at 120 °C for 1 h. (C) SAED pattern and (D) HRTEM of $CH_3NH_3PbI_3$ prepared with reaction time of 1 h.

the crystal structure and morphology of the as-prepared $CH_3NH_3PbI_3$ crystal. Figure 1B shows the typical PXRD patterns of the resulting products, and the main diffraction peaks, assigned to the (110), (220), (310) and (330) peaks at 2θ = 14.18°, 28.47°, 31.93° and 43.28° can be indexed to those reported in the literatures,[23, 24] which indicates that this one-step solution process technique is an effective method to produce the $CH_3NH_3PbI_3$ perovskites single crystals. From the PXRD patterns, it can be concluded that, as the reaction temperature increased, the crystallinity of the products is indeed increased gradually with the reaction temperature. PXRD of the perovskite crystals sustaining different reaction time is shown in Figure S1. Transmission electron microscope (TEM) characterized the microstructure of the $CH_3NH_3PbI_3$ single crystals for 1 h. The single crystal characteristic was illustrated by selected area electron diffraction (SEAD) pattern depicted in Figure 1C, as the side surface should be a (100) facet and the head surface should be a (001) facet. In the HRTEM image, a crystalline structure with a lattice spacing of 0.31 nm can be indexed to (004) or (220) of the tetragonal $CH_3NH_3PbI_3$ phase (Figure 1D).[25]

To understand the formation mechanism and dissolving effect of these perovskite cuboid crystals, time-dependent experiments were carried out. An interesting structural evolution process from solid microcuboids to hollow cuboid microframes was observed in Figure 2. SEM investigations show that the products after reaction of 0.5 h are cuboid aggregates consisting of primary nanoparticles with size between 80 and 150 nm (Figure 2A). The oriented aggregation phenomenon in the process of the crystal growth could be observed from the Figure 2A. With prolonged reaction time to 1 h, the SEM observations (Figure 2B) showed that the majority of perovskite particles appeared as cubic crystallites of smaller size between ~1 and ~4 μm after 1 h of crystallization in Figure 2B. In the process of subsequent growth small crystals dissolved and redeposited onto the surface of larger crystals. This phenomenon indicates that Ostwald ripening is an underlying mechanism operative in this growth process. This is understandable, because there is chemical species to generate necessary ionic transport in solution during the ripening process.[26] On the whole the crystal shape of the perovskite crystals for 4 h (Figure 2C) has no significant change compared to the starting samples but with a much larger size. All these crystal surfaces present the thermodynamic stable cuboid shape enclosed by the flat surfaces. When the reaction time increased to 6 h, it can be clearly observed that small etching traces and inverted pyramidal pits (Figure 2D) were generated on (001) surfaces. By prolonging the treating time to 24 h, the small pits on the facet evolve into a significant etching even appearing the etching steps. As shown in Figure 2E, the as-synthesized crystals well retain the cuboid shape, while the size has decreased to about 12 μm. As the reaction continued, a shallow hole was emerged after reaction for 36 h (Figure 2F), which became deeper on all of the faces of the crystal. At last cuboids are etched from every fact forming a hollowed-out skeleton, and the whole skeleton even collapses into tetrahedrons (Figure S2 and S3).

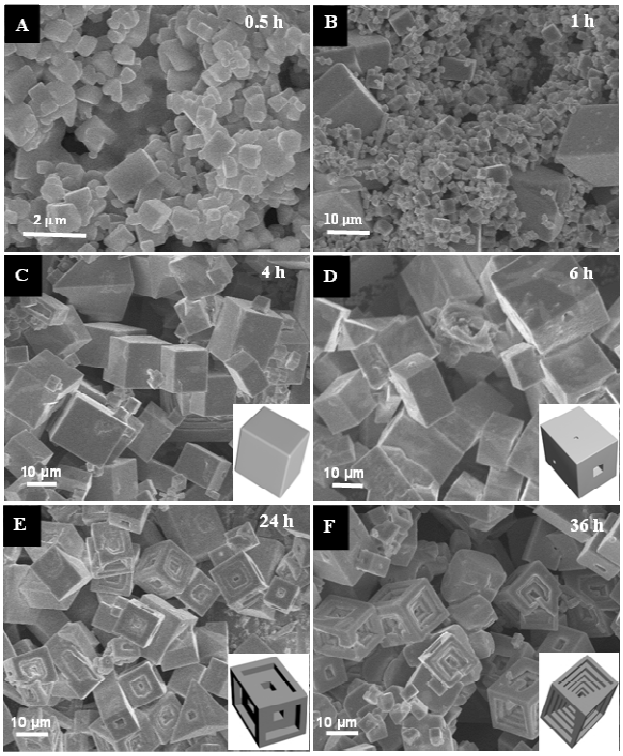

Figure 2. $CH_3NH_3PbI_3$ products prepared with different reaction time: A,B,C,D,E and F for 0.5 h, 1 h, 4 h, 6 h, 24 h and 36 h respectively.

Recently studies have shown that the reaction temperature is the one of keys to being able to predictably control the crystal and film growth.[20, 27] In order to explore the effects of crystallization process at the different temperatures, specimens were collected after crystal growth temperatures of 60 °C, 100 °C, 120 °C, 140 °C, and 160 °C for 12 h. The influence of the reaction temperature on the morphology and structure of the perovskite crystals synthesized by one-step solvothermal were examined by SEM (Figure 3). The samples prepared at 60 °C show irregular shape with the crystal size of 1~2 μm. When the reaction temperature is at 100 °C, the average cuboid size was increased with the reaction temperature rising, which is about 14 μm. At the stage the obtained product exhibits an identical structure to the starting material without any etching

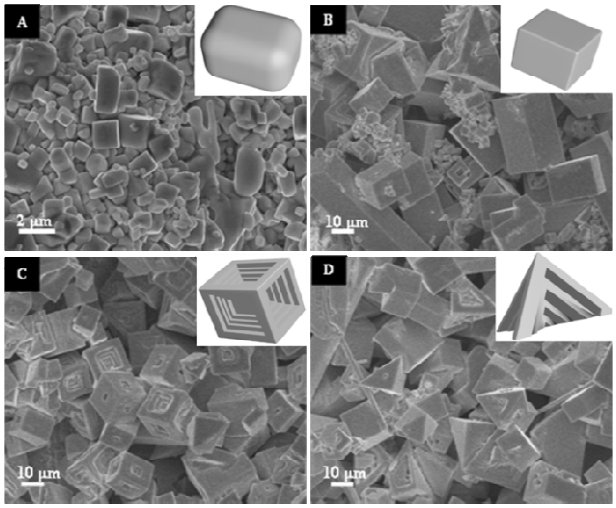

Figure 3. $CH_3NH_3PbI_3$ crystals with different reaction temperatures: (A), (B), (C) and (D) correspond to 60 °C, 100 °C, 140 °C and 160 °C. The reaction time of all the samples is 12 h.

traces detected on the crystal surfaces. Nevertheless, further increasing the reaction temperature leads to significant etching phenomena on the surfaces of the resulting products. Furthermore, the facial etching gradually intensified as the temperature increased, which can be deduced from the SEM images shown in Figure 3C and 3D. With the temperature increasing, the etching of facets is so violent that the whole cuboid perovskite crystals broke into tetrahedrons and other blocks in Figure 3D.

In addition, the grain size distribution graphs of the products on the condition of different reaction time and temperature were presented in Figure 4. Due to the dissolving effect, grain size distribution is not monotonic increase along with the prolonging of the time and the rising of the temperature. From the reaction time-grain size distribution graph (Figure 4A), the grain size reached the maximum about 25 μm for 10 h. And the optimal temperature to obtain the large crystals is 120 °C for 12 h. In other words, the prolonged reaction time and the increased reaction temperature accelerated the dissolving process. The dissolving effect not only led to the etching of the crystallographic planes but also decreased the crystals size.

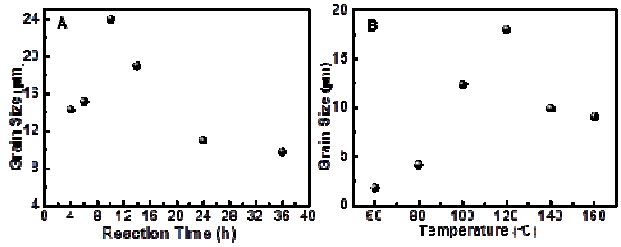

Figure 4. (A) The reaction time dependence of grain size in $CH_3NH_3PbI_3$ crystals. (B) The temperature dependence of grain size in $CH_3NH_3PbI_3$ crystals.

In the present synthesis strategy, the long reaction time and higher reaction temperature will lead to dissolving of the $CH_3NH_3PbI_3$ crystals. This finding indicates that the structure-induced anisotropic chemical etching/dissolving of $CH_3NH_3PbI_3$ is highly dependent on the reaction time and temperature. The substantial stability for the hybrids derives from the specific range of chemical interactions found in these systems—from relatively weak van der Waals interactions among the organic components, to hydrogen bonding interactions between the organic and inorganic components (as well as among the organic molecules), and stronger ionic and covalent interactions within the metal halide sheets.[28] The perovskite crystals belong to cubic phase (space group Pm3m, Z=1) at the reaction temperature 120 °C exceeding the phase transition point of 54 °C. The $CH_3NH_3^+$ is fully disordered due to the cubic symmetry. The ammonium group on each $CH_3NH_3^+$ hydrogen bonds to halogens in the perovskite structure.[29] These specific hydrogen bonding interactions and the constraints imposed by the distorted perovskite framework in $CH_3NH_3PbI_3$ stabilize the conformation. High reaction temperature and long reaction time will lead to the dissolving of the perovskite crystals. With increasing temperature, the lattice constants a and c increases monotonically.[30, 31] This will lead the intense rotation of the $CH_3NH_3^+$ and the weakness of the hydrogen bonding. Meantime as the reaction continues, low super-saturation of the perovskite precursors made as-synthesized crystals dissolve. The lateral sides expected with more defects and the gathering of the dislocations compared to the smooth edges, which provide more reactive sites for dissolving.[31] It led to a higher stability at the corners and edges than at the centre of the faces.

Ostwald ripening involves in both steps, providing substance for recrystallization.[32] The oriented aggregation of the initial small particles is important for the continuous morphology transition as it allows easy fusion between centre and ledge that have aligned in the same crystallographic direction. It is observed the interior of $CH_3NH_3PbI_3$ single crystals is constructed by small microparticles, as seen in Figure S4. The surfaces of the samples preserved in the humidity of sixty percent for 3 h have been decomposed. While during the process of dissolving, the surfaces of the crystals retained smooth. Therefore the dissolving is dynamic balance process of dissolving and recrystallization. And Ostwald ripening mechanism does exist in the experimental process.

We then measured the UV–vis absorption and photoluminescence (PL) of the obtained $CH_3NH_3PbI_3$ perovskite crystals at room temperature as depicted in Figure S5. $CH_3NH_3PbI_3$ crystals we synthesized display a strong, abrupt absorption in the visible spectral region and have broad optical absorption up to 800 nm.[9] The time dependence of the PL intensity demonstrated that as the reaction time increased, the defects of the products decreased.[33] Therefore, it is not surprising that the emission properties receded with the reaction time prolonged.

In summary, we have developed a one-pot solvothermal synthesis strategy to prepare large $CH_3NH_3PbI_3$ perovskite single crystals for revealing the intrinsic crystal growth mechanism. The method allows controlling over grain growth of $CH_3NH_3PbI_3$ and the process of dissolving, and achieves the rapid and reproducible fabrication of well-defined perovskite single crystals. We elaborated stability of the crystal by the crystallization and dissolving process under the solvothermal condition. It is presented that the higher temperature and longer reaction time can affect the crystallization of the perovskite crystals and lead to the exposure of the high-index facets in the isopropanol solution. There is a higher stability at the corners and edges than at the centre of the faces. In a word this

synthetic technology will not only benefit the perovskite based photovoltaic devices but also bring new possibilities to perovskite-based hybrid optoelectronic devices, such as field effect transistors and light emitting diodes.

Notes and references

1 D. B. Mitzi, in Progress in Inorganic Chemistry, John Wiley & Sons, Inc. 2007, pp. 1-121.
2 A. Kojima, K. Teshima, Y. Shirai and T. Miyasaka, *J. Am. Chem. Soc.*, 2009, **131**, 6050.
3 J.-H. lm, C. R. Lee, J. W. Lee, S. W. Park, N. G. Park, *Nanoscale*, 2011, **3**, 4088.
4 H. S. Kim, C. R. Lee, J. H. Im, K. B. Lee, T. Moehl, A. Marchioro, S. J. Moon, R. Humphry-Baker, J. H. Yum, J. E. Moser, M. Gratzel, N. G. Park, *Sci Rep*, 2012, **2**, 591.
5 J. Burschka, N. Pellet, S. J. Moon, R. Humphry-Baker, P. Gao, M. K. Nazeeruddin, M. Gratzel, *Nature*, 2013, **499**, 316-319.
6 N. J. Jeon, J. H. Noh, W. S. Yang, Y. C. Kim, S. Ryu, J. Seo, S. I. Seok, *Nature*, 2015, **517**, 476.
7 M. D. McGehee, *Nat. Mater.*, 2014, **13**, 845.
8 M. Z. Liu, M. B. Johnston, H. J. Snaith, *Nature*, **501**, 395-398.
9 S. Yang, Y. C. Zheng, Y. Hou, X. Chen, Y. Chen Y. Wang, H. J. Zhao, H. G. Yang, *Chem. Mater.*, 2014, **26**, 6705.
10 H. Zhou, Q. Chen, G. Li, S. Luo, T. B. Song, H. S. Duan, Z. Hong, J. You, Y. Liu, Y. Yang, *Science*, 2014, **345**, 542.
11 Z. -K. Tan, R. S. Moghaddam, M. L. Lai, P. Docampo, R. Higler, F. Deschler, M. Price, A. Sadhanala, L. M. Pazos, D. Credgington, F. Hanusch, T. Bein, H. J. Snaith, R. H. Friend, *Nat. Nano.*, 2014, **9**, 687.
12 G. Xing, N. Mathews, S. S. Lim, N. Yantara, X. Liu, D. Sabba, M. Gratzel, S. Mhaisalkar, T. C. Sum, *Nat. Mater.*, 2014, **13**, 476.
13 F. Deschler, M. Price, S. Pathak, L. E. Klintberg, D.-D. Jarausch, R. Higler, S. Hüttner, T. Leijtens, S. D. Stranks, H. J. Snaith, M. Atatüre, R. T. Phillips, R. H. Friend, *J. Phys. Chem. C.*, 2014, **5**, 1421.
14 B. R. Sutherland, S. Hoogland, M. M. Adachi, C. T. O. Wong, E. H. Sargent, *ACS Nano*, 2014, **8**, 10947.
15 Q. Dong, Y. Fang, Y. Shao, P. Mulligan, J. Qiu, L. Cao, J. Huang, *Science*, 2015, **347**, 967.
16 H. Zhu, Y. Fu, F. Meng, X. Wu, Z. Gong, Q. Ding, M. V. Gustafsson, M. T. Trinh, S. Jin, X. Y. Zhu, *Nat. Mater.*, 2015, doi:10.1038/nmat4271
17 Y. Fu, F. Meng, M. B. Rowley, B. J. Thompson, M. J. Shearer, D. Ma, R. J. Hamers, J. C. Wright, S. Jin, *J. Am. Chem. Soc.*, 2015, **137**, 5810.
18 S. Zhuo, J. Zhang, Y. Shi, Y. Huang, B. Zhang, *Angew. Chem. Int. Ed.*, 2015, **127**, 5785.
19 G. Xing, N. Mathews, S. Sun, S. S. Lim, Y. M. Lam, M. Gratzel, S. Mhaisalkar, T. C. Sum, *Science*, 2013, **342**, 344.
20 G. E. Eperon, V. M. Burlakov, P. Docampo, A. Goriely, H. J. Snaith, *Adv. Funct. Mater.*, 2013, **24**, 151.
21 D. Shi, V. Adinolfi, R. Comin, M. Yuan, E. Alarousu, A. Buin, Y. Chen, S. Hoogland, A. Rothenberger, K. Katsiev,Y. Losovyj, X. Zhang, P. A. Dowben, O. F. Mohammed, E. H. Sargent, O. M. Bakr, *Science*, 2015, **347**, 519.
22 W. Nie, H. Tsai, R. Asadpour, J. C. Blancon, A. J. Neukirch, G. Gupta, J. J. Crochet, M. Chhowalla, S. Tretiak, M. A. Alam, H. -L. Wang, A. D. Mohite, *Science*, 2015, **347**, 522.
23 T. Baikie, Y. Fang, J. M. Kadro, M. Schreyer, F. Wei, S. G. Mhaisalkar, M. Graetzel, T. J. White, *J. Mater. Chem. A*, 2013, **1**, 5628.
24 M. Liu, M. B. Johnston, H. J. Snaith, *Nature*, 2013, **501**, 395.
25 M. Xiao, F. Huang, W. Huang, Y. Dkhissi, Y. Zhu, J. Etheridge, A. Gray-Weale, U. Bach, Y. B. Cheng, L. Spiccia, *Angew. Chem. Int. Ed.*, 2014, **126**, 10056.
26 H. G. Yang, H. C. Zeng, *J. Phys. Chem. B*, 2004, **108**, 3492.
27 A. Dualeh, N. Tétreault, T. Moehl, P. Gao, M. K. Nazeeruddin, M. Grätzel, *Adv. Funct. Mater.*, 2014, **24**, 3250.
28 D. B. Mitzi, *J. Chem. Soc., Dalton Trans.*, 2001, 1.
29 Y. Kawamura, H. Mashiyama, K. Hasebe, *J. Phys. Soc. Jpn.*, 2002, **71**, 1694.
30 A. Poglitsch, D. Weber, *J. Chem. Phys.*, 1987, **87**, 6373.
31 W. R. Wilcox, *J. Cryst. Growth*, 1977, **37**, 229.
32 J. Li, S. Hietala, X. Tian, *ACS Nano*, 2015, **9**, 496.
33 C. C. Stoumpos, C. D. Malliakas, M. G. Kanatzidis, *Inorg. Chem.*, 2013, **52**, 9019.

TOC Image：

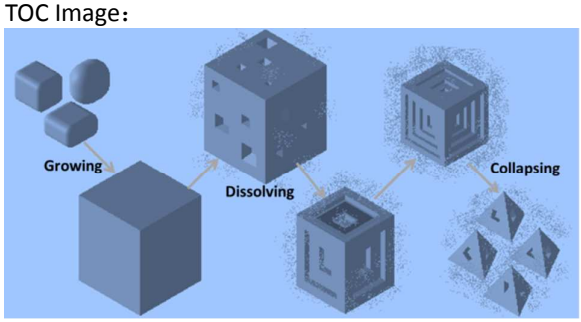

A one-pot solvothermal approach to synthesize the cuboid shaped $CH_3NH_3PbI_3$ single crystals was reported. The growing and dissolving phenomenon of perovskite crystals was discovered under the solvothermal condition. It is crucial to explore the crystallization and stability of perovskites.